A-6

2nd
IEEE MEDITERRANEAN SYMPOSIUM ON NEW DIRECTIONS IN CONTROL & AUTOMATION

JUNE 19 - JUNE 22, 1994

MALEME BEACH HOTEL
(CRETE CHANDRIS HOTEL)

MALEME, CHANIA
CRETE
GREECE

IEEE

CSS

Technical Co-Sponsors:

IEEE Control Systems Society
IEEE Robotics & Automation Society

Financial Sponsors:

THE GREEK CHAPTER OF THE IEEE CONTROL SYSTEMS SOCIETY
TECHNICAL UNIVERSITY OF CRETE
ΓΓΕΤ (GENERAL SECRETARIAT FOR RESEARCH AND DEVELOPMENT)
UNIVERSITY OF PATRAS
THE UNIVERSITY OF SOUTHWESTERN LOUISIANA

NASA-CR-203134

Gasdynamics and Transport in a High-pressure Reactor under Microgravity Conditions *

H. T. Banks, K. Ito, J. S. Scroggs† and H. T. Tran
Center for Research in Scientific Computation
Department of Mathematics
North Carolina State University
Raleigh, NC 27695 USA
and
K. J. Bachmann, H. Castleberry, and S. Feichter
Department of Materials Science and Engineering
North Carolina State University
Raleigh, NC 27695 USA

Abstract

The coupled gas-phase chemical kinetics and fluid mechanics in a vertical reactor for high pressure vapor transport (HPVT) of compound semiconductors are modeled. The modeling is for the growth of II-IV-V_2 chalcopyrite $ZnGeP_2$ and addresses the flow of dense phosphorus gas at 3.5 atmospheric pressure. The mathematical model for transport processes is described by conservation of mass, momentum, energy, and mass transfer equations; in addition, buoyancy effects are included in the model through the gravitational term in the momentum equation. The complete model incorporates multiple species, thermal diffusion effects, and gas-phase chemical reactions. Calculations of fluid/thermochemical data such as density, viscosity, thermal conductivity, heat capacity, mass diffusion coefficients, rate constants and activation energies of the gas reactions are discussed. Numerical results of a 2-D, steady, axi-symmetrical flow are presented using a finite element discretization with non-uniform, rectangular elements. The numerical simulations were performed to study the effects of gravitational-induced buoyancy-driven convection flows in HPVT crystal growth.

*This work was supported by National Aeronautics and Space Administration grant #NAGW-2865.

†scroggs@wave.math.ncsu.edu

1 Introduction

Non-linear optical interactions in birefringent materials find applications in phase-matched harmonic generation and frequency mixing. In particular, $ZnGeP_2$, which has a high non-linear susceptibility coefficient, has been used for manufacturing frequency agile infrared lasers and second harmonic generation (SHG) of infrared (CO_2 laser) radiation. Typically, these materials have been processed using bulk crystal growth techniques (solidification); however, there are several shortcomings to this processing method. Namely, residual absorption within its transparency range due to impurities and native defects limits the performance and lowers the laser damage threshold of $ZnGeP_2$ non-linear optical devices that are built with bulk single crystals, thus in-plane non-linear interactions in high quality heteroepitaxial films become an attractive alternative. In addition, heteroepitaxial structures generally provide for greater beam coherency lengths than achievable with bulk single crystals.

Fluid dynamics limitations to the uniformity of deposition and etching processes have been overcome by operating at low vapor densities. However, some of the most important applications pertain to infrared laser sources which require μm thick films. This mandates epitaxial deposition at rates higher than those which

can be achieved at low densities. Because the control of fluid dynamics is essential for processes operating at high flows or vapor densities, advanced methods of mathematical modeling, optimization, and control theory will be applied to guide the experimental implementation of theses processes. We address the application-driven research to develop mathematical models based on gas-dynamics equations which accurately describe gas flow and deposition processes for HPVT reactors and state-of-the-art computational algorithms to construct optimal control synthesis for regulation of epitaxial deposition process operating at high vapor densities. The first stage in this process is the development of robust and accurate (numerical) simulations of the dominant physical phenomenon governing the fluid dynamics as presented here.

We have previously discussed the thermochemical properties of $ZnGeP_2$ taking into account all thermodynamical data available [4]. These calculations allow a prediction of the composition and the densities of the vapor phase, of which are needed as input data for modeling the gas flow dynamics and heat transfer of HPVT. In addition, calculations related to the activation energies and rate constants of the reactions

$$P_4 \rightleftharpoons 2P_2$$

were also presented. In this manuscript we help complete the list of necessary parameters by presenting a detailed discussion of calculations of mass diffusion coefficients. Studies have also been made concerning the choices that need to be made in the thermal boundary conditions to optimize the vapor transport from the source and to establish uniform flow at the surface of the substrate[1]. In addition to the parameter studies, a more rigorous approach to the optimal design and control has been taken. In [7] the shape optimization problem with respect to the geometry of the reactor and a boundary temperature control problem were formulated. The material and shape derivatives of solutions to the Boussinesq approximation were derived. Optimality conditions and a numerical optimization method based on the augmented Lagrangian method were developed for boundary control of Boussinesq flow. Numerical calculations in [6] indicated the effectiveness of temperature control through a portion of the boundary for improving the vertical transport of flow in the cavity.

This paper addresses the issue of a reduction in the convective effects by growing the material under reduced gravity (microgravity) conditions. Numerical calculations of the flow dynamics show a formation of additional vortices and an increase in the flow velocity as one changes from microgravity (1/1000– g) condition to terrestrial gravitational field. Our preliminary qualitative comparision with experiments at 1 g indicate that numerical simulations can correctly describe physical phenomena occuring in HPVT reactor. However, more rigorous tests are needed to confidently validate numerical experiments.

2 HPVT Experiment

A modified Scholz geometry ampoule was used for the growth experiments of $ZnGeP_2$. A cross section of the growth flow area is depicted in Fig. 1. The source material and the growing crystal are hermetically sealed in fused silica ampoule (with vertical height of 8.3cm and maximum radial width of 2.3cm) that is located in a furnace A ring-shaped booster heater at the source permits its heating to a temperature above that of the outer cylindrical surface. Connected to the center of the ampoule is a fused silica tube, terminating in a flat fused silica window, from which heat can be extracted in a controlled manner by a jet of nitrogen gas directed onto its outer surface. Due to the lower temperature at this window, the $ZnGeP_2$ transport can be modeled via evaporation from the hot source and condenses on the cooled window. The top dome surface of the ampoule can be either heated to the same temperature as the side faces by use of a closed furnace liner or be kept cooler than the side faces by another jet of nitrogen onto its outer surface.

HPVT experiments have been conducted for $ZnGeP_2$ in this ampoule and in conventional horizontal quartz tubes. Thus far, the largest crystals have been obtained in horizontal ampoules where the $ZnGeP_2$ transport flux was of the order 5×10^{-6} mole/m^{2}sec at $1300K$ and $1 - ga$ [4].

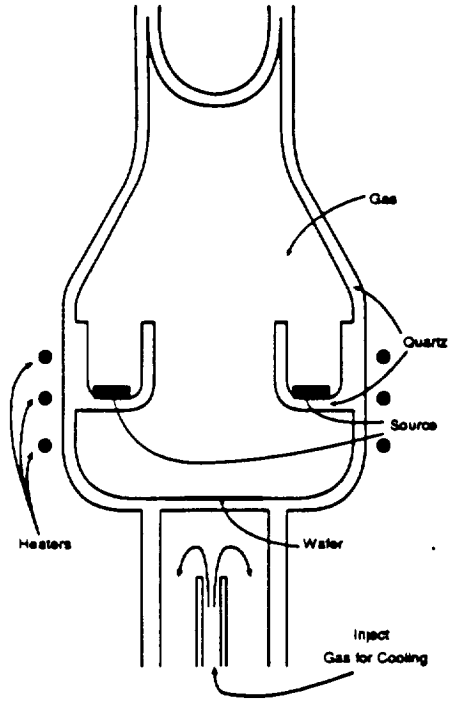

Figure 1: Schematic of the growth section of the Scholz-type geometry ampoule

3 Mathematical Formulation

3.1 Description of Model

The mathematical model for the transport phenomena involved in the HPVT process couples the usual gasdynamic equations (conservation of mass, momentum and energy) with an equation for the effects of species diffusion. However, since the film growth rate is slow compared to the gas-phase dynamics, the gas flow can be accurately modeled even if the deposition is not coupled with the flow. The flow is assumed to be a steady-state flow. We also assume that the flow is laminar, Newtonian, and axi-symmetric (i.e. all field quantities are independent of θ and $u_\theta = 0$). These simplified equations in cylindrical coordinates are:

Mass

$$\frac{1}{r}\frac{\partial}{\partial r}(\rho r u_r) + \frac{\partial}{\partial z}(\rho u_z) = 0.$$

Momentum

$$\begin{aligned}
\rho\left(u_r\frac{\partial u_r}{\partial r} + u_z\frac{\partial u_r}{\partial z}\right) &= \frac{1}{r}\left(\frac{\partial}{\partial r} r\sigma_{rr}\right) \\
&- \frac{1}{r}\sigma_{\theta\theta} + \frac{\partial \sigma_{rz}}{\partial z}, \\
\rho\left(u_r\frac{\partial u_z}{\partial r} + u_z\frac{\partial u_z}{\partial z}\right) &= \frac{1}{r}\left(\frac{\partial}{\partial r} r\sigma_{rz}\right) \\
&+ \frac{\partial \sigma_{zz}}{\partial z} + (\rho - \rho_0)g,
\end{aligned}$$

where the stress tensor $\sigma_{rr} = -p + 2\mu\frac{\partial u_r}{\partial r}$, $\sigma_{\theta\theta} = -p + 2\mu\frac{u_r}{r}$, $\sigma_{rz} = \mu\left(\frac{\partial u_r}{\partial z} + \frac{\partial u_z}{\partial r}\right)$, and $\sigma_{zz} = -p + 2\mu\frac{\partial u_z}{\partial z}$.

Energy

$$\begin{aligned}
\rho c_p\left(u_r\frac{\partial T}{\partial r} + u_z\frac{\partial T}{\partial z}\right) &= \frac{1}{r}\frac{\partial}{\partial r}\left(kr\frac{\partial T}{\partial r}\right) \\
&+ \frac{\partial}{\partial z}\left(k\frac{\partial T}{\partial z}\right).
\end{aligned}$$

Species

$$\begin{aligned}
\rho\left(u_r\frac{\partial c_i}{\partial r} + u_z\frac{\partial c_i}{\partial z}\right) &= \frac{1}{r}\frac{\partial}{\partial r}\left(\rho\alpha_1 r\frac{\partial c_i}{\partial r}\right) \\
&+ \frac{\partial}{\partial z}\left(\rho\alpha_1\frac{\partial c_i}{\partial z}\right) + R_i.
\end{aligned}$$

Here u_r, u_z, p, g, T, c_i and R_i are radial and axial velocities, pressure, gravity, temperature, species concentration (expressed as mass fraction) of the i'th specie, and chemical reaction rate, respectively. In the above formulation we assume that the fluid is compressible and that the density varies with temperature and species concentration, but is independent of pressure. That is the density is represented in the form

$$\rho = \frac{\rho_0[1 - \beta_T(T - T_0)]}{1 + \sum_{n=1}^{N-1}(M_N/M_n - 1)c_n},$$

where ρ_0, T_0 are reference values, β_T is the coefficient of volumetric expansion associated with temperature variations, M_n is the molecular weight of the n'th component, and the component N is considered to be the carrier gas. Finally, μ is the (dynamic) viscosity, k is coefficient of heat conductivity, c_p is the specific heat, and α_1 is the mass diffusion coefficient.

It should be noted that currently the buoyancy force arising from density variations was

included in the momentum equation as the term $(\rho - \rho_0)g$. Future modeling efforts will include thermal (Soret) diffusion of the species since this effect is expected to be significant with the large spatial temperature variations of this experiment (see e.g. [8] and the references given therein).

The boundary conditions used in our numerical experiments are:

- no slip except along the axis of symmetry where $u_r = 0$ and u_z is free;
- experimentally measured wall temperature profiles; that is, constant $T = 1298°$K along most of the boundary except for the following two locations: (i) T is a piecewise cubic Hermite interpolant that satisfies $T(z = .043) = 1348°$K at the top of the trough, and $T(z = .043 \pm .01825) = 1298°$K; in addition, (ii) along the bottom of the ampoule, where the substrate is cooled by helium, $T = 1223°$K for $0 < r < .0057$, and T is a linear function satisfying $T(r = .0057) = 1223°$K and $T(r = .0092) = 1298°$K;
- zero flux of reactants except at the source where mass concentrations are constant.

Note that the temperature boundary conditions are applied on the outside of the quartz chamber, and that the no-slip and flux boundary conditions are applied on the inside of the chamber.

3.2 Parameters

As discussed earlier, a melt of the compounds was used as the source for vapor phase growth. However, heating of $ZnGeP_2$ in an evacuated, closed system causes thermal decomposition of the material. We determine the vapor phase composition of $ZnGeP_2$ at the melting point, $T = 1295°$ K, via Gibbs free energy minimization techniques (see [4, 3]) and the result is summarized in Table 1.

From the data in Table 1, we concluded that the gas phase is dominated by P_4 (and some P_2) gas. Based on this, the numerical experiments use the assumption that the gas phase

Gas Species	Density mole/cm^3	Pressure bar
P_4	7.61×10^{-5}	2.77
P_2	1.05×10^{-5}	3.81×10^{-1}
Zn	6.27×10^{-6}	2.28×10^{-1}
Ge	4.47×10^{-13}	1.63×10^{-8}
Total	9.29×10^{-5}	3.38

Table 1: Contents of gas phase at 1295° K

consists of only P_4 and P_2. In addition, the values in Table 1 provide us the weights used to determine the fluid dynamic properties with data taken from [9]. Thus, we use $\rho_0 = 4.0629$ kg/m^3 and $T = 1300°$ K for the refence density and temperature, $\mu = 2.699 \times 10^{-5}$ m^2/s for the viscosity, $k = 2.301 \times 10^{-2}$ J/m − s − K for the coefficient of heat conduction, and $c_p = 600.7$ J/kg − K. And for the values used in boundary conditions for mass concentrations at the source we employed 0.9372 for P_4 and 0.0628 for P_2. Based on data from Table 1, we also assume that the mean operating pressure is 3.5 atm. It should be noted that in this model the transport properties are constant. However, when there is a large variation in temperature these properties undergo significant changes during the flow and should be accounted for in any realistic growth simulation.

The mass diffusivity α_1 for binary mixtures is computed from the Chapman-Enskog theory [2]. For gaseous state at low density, the formula for α_1 is given by

$$\alpha_1 = 18.583 \frac{\sqrt{T^3 \left(\frac{1}{M_1} + \frac{1}{M_2}\right)}}{p\sigma_{12}^2 \Omega_{12}} \qquad (1)$$

in which $T = 1300°$ K, $M_1 = 123.880$ is the mass concentration of P_4, $M_2 = 61.940$ is the mass concentration of P_2, and $p = 3.5$ atm. The Lennard-Jones parameter σ_{12} is computed as the average of the Lennard-Jones parameters of P_4

and P_2:

$$\sigma_{12} = \frac{1}{2}(\sigma_{P2} + \sigma_{P4}),$$

where $\sigma_{P2} = 3.03$ Å and $\sigma_{P4} = 4.90$ Å [5]. Finally, Ω_{12} is a dimensionless function of the temperature and of the intermolecular potential field for one molecule of P_2 and one molecule of P_4. From [2], this potential field can be approximated by the Lennard-Jones function:

$$\varphi_{12}(r) = 4\epsilon_{12}\left[\left(\frac{\sigma_{12}}{r}\right)^{12} - \left(\frac{\sigma_{12}}{r}\right)^{6}\right].$$

In our calculations, we compute the potential energy function by linear interpolation ([2], Table B-2). This function is given as a function of Tk/ϵ_{12} where

$$\frac{\epsilon_{12}}{k} = \sqrt{\left(\frac{\epsilon}{k}\right)_{P2}\left(\frac{\epsilon}{k}\right)_{P4}}.$$

Using $\left(\frac{\epsilon}{k}\right)_{P2} = 653^oK$ and $\left(\frac{\epsilon}{k}\right)_{P4} = 711^oK$ (from [9]) gives $Tk/\epsilon_{12} = 1.9079$ and from ([2], Table B-2) we then obtain $\Omega_{12} = 1.0924$. Substitution of the foregoing values into equation (1) gives

$$\alpha_1 = 2.2550 \times 10^{-5}$$

4 Numerical Results

The coupled gasdynamic equations from §3.1 were solved numerically with the above mentioned boundary conditions using a finite-element code FIDAP with nonuniform, rectangular elements. The computations were performed on an IBM RISC/6000 model 340 and the CPU times for a typical 2D case (15,500 unknows) were 3-5 hours. We have compared the numerical results of coarse grids to fine grids and they are differed by less than 1%. Therefore, we are confident that the transport phenomena obtained below are resolved.

Numerical experiments were performed to study the effects of gravitationally-induced buoyancy driven convection flows on the quality of the crystal growth. In the following flow calculations, the Reynold number is 5.56. In addition, the Prandtl number is 2.86 and the Grashof number is 7.24×10^2, thus it is reasonable to expect the flow to be time-independent.

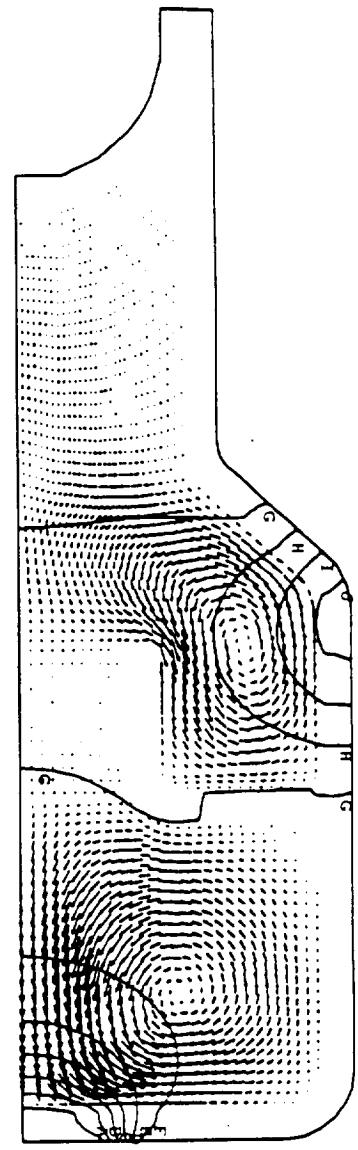

Figure 2: Vel. and Temp. at 1/1000 gravity of sea level

In Fig. 2, we show an overlay of the temperature contours with the velocity fields at 1/1000 sea level gravity. In this figure, we have a maximum velocity of 0.1828×10^{-1} cm/s, maximum

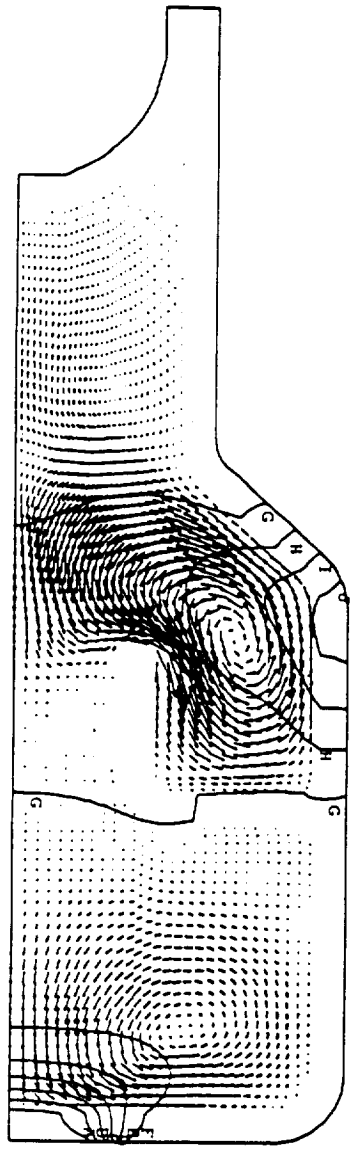

Figure 3: Vel. and Temp. at 1/10 gravity of sea level

temperature equals 1348°K, minimum temperature equals 1223°K and the temperature contours with scale given in Table 2.

In the plot showing velocity fields, the length of the velocity vectors provides a measure of the relative velocity magnitude. The calculations show the convective mixing over the annular source region and downward laminar flow over the substrate surface.

A	1229
B	1242
C	1254
D	1267
E	1279
F	1292
G	1304
H	1317
I	1329
J	1342

Table 2: Scales for temperature contours

An overlay of the temperature contours with the velocity fields at 1/10 sea level gravity are depicted in Fig. 3. In this figure, we have a maximum velocity of .8868 cm/s, maximum temperature equals 1348°K, minimum temperature equals 1223°K and the temperature contours with scale given in Table 2. Here, we observe the formulation of a third convective roll near the top plug which could help explain the occurence of small crystallites observed in that area in our physical experiments. A comparison of the 1/10-g and 1/1000-g cases in this study indicates that the buoyancy effects are, indeed, suppressed in microgravity condition. The subtle differences between the $1g$ and μg cases and how they may be important in HPVT processes will be the subject of future study.

References

[1] K. Bachmann, G.-C. Xing, J. Scroggs, H. Tran, K. Ito, H. Castleberry, and G. Wood, *Heteroepitaxy of wide bandgap ternary semiconductors*, Japanese Journal of Applied Physics, in print (1994).

[2] R. B. Bird, W. E. Stewart, and E. N. Lightfoot, *Transport Phenomena*, John Wiley & Sons, New York, 1960.

[3] G. Eriksson and K. Hack, *Chemsage–a computer program for the calculation of com-*

plex chemical equilibria, Metallurgical Transactions B, 21B (1990).

[4] S. FIECHTER, R. CASTLEBERRY, G. WOOD, K. BACHMANN, H. TRAN, K. ITO, AND J. SCROGGS, *High pressure vapor transport of binary and ternary compound semiconductors*, in Proceedings of the Sixth International Symposium on Experimental Methods for Microgravity Materials Science, TMS, 1994, p. to appear.

[5] H.-U. FINZEL, *Transport of Zn_3P_2 by vapor phase transport*, J. Crystal Growth, 50 (1980), pp. 823–830.

[6] K. ITO, J. SCROGGS, AND H. TRAN, *Optimal control of thermally coupled Navier-Stokes equations*, SIAM J. Opt., (submitted).

[7] ——, *Optimal design of a vapor transport reactor*, in Proceedings of the IMA Workshop on Flow Control, Minnesota, to appear, IMA.

[8] J. OUAZZANI AND F. ROSENBERGER, *Three-dimensional modeling of horizontal chemical vapor deposition I. MOCVD at atmospheric pressure*, J. Crystal Growth, 100 (1990), pp. 545–576.

[9] R. A. SVEHLA, *Estimated viscosities and thermal conductivities of gases at high temperatures*, Technical Report NASA TR R-132, NASA, Washington, D.C., 1962.